Selective Formation of Rare-Earth–Nickel Alloys via Electrochemical Reactions in NaCl–KCl Molten Salt

Kouji Yasuda[a,b,*,z], Katsuya Kondo[a], Seitaro Kobayashi[a],

Toshiyuki Nohira[a,c,*,z], Rika Hagiwara[a,*]

a: Graduate School of Energy Science, Kyoto University,

Yoshida-honmachi, Sakyo-ku, Kyoto 606-8501, Japan

b: Environment, Safety and Health Organization, Kyoto University,

Yoshida-honmachi, Sakyo-ku, Kyoto 606-8501, Japan

c: Present address: Institute of Advance Energy, Kyoto University,

Gokasyo, Uji 611-0011, Japan

*Electrochemistry Society Active Member

[z]E-mail: yasuda.kouji.3v@kyoto-u.ac.jp, nohira.toshiyuki.8r@kyoto-u.ac.jp

Tel: +81-75-753-4817

Fax: +81-75-753-5906

Abstract

Toward the establishment of the electrochemical recovery process of rare-earth (RE) elements from used magnet scraps, selective electrochemical formation of RE–Ni alloys (RE = Pr, Nd, and Dy) was investigated in molten NaCl–KCl–$NdCl_3$–$DyCl_3$ and NaCl–KCl–$PrCl_3$–$NdCl_3$–$DyCl_3$ at 973 K. Alloy samples were prepared by potentiostatic electrolysis using Ni plate electrodes at various potentials. The compositions of the formed alloys were analyzed using energy-dispersive X-ray spectroscopy (EDX), and the separation factors defined as $\{x_{Dy}/(x_{Pr} + x_{Nd})\}_{alloy}$ were compared. High separation factors of 9.9 and 22.9 were obtained at 0.42 V and 0.45 V (vs. Na^+/Na), respectively, indicating the possibility of effective separation and recovery of REs from the used magnet scraps. The optimum electrolysis condition was studied based on the discussion on the formation mechanism of RE–Ni alloys.

Keywords

Rare earth, Recycling, Molten salt, NaCl–KCl

1. Introduction

The use of rare-earth (RE) elements is essential for recent high-functional devices. Typical examples in energy fields include permanent magnets, fluorescent substances, light-emitting diodes (LEDs), solid electrolytes, and hydrogen storage alloys. In particular, neodymium–iron–boron (Nd–Fe–B) magnets, or so-called neodymium permanent magnets, are used for voice coil motors (VCM) in hard disk drives (HDDs), speakers/vibrators in cellular phones, and motors in electric vehicles (EVs) and hybrid electric vehicles (HEVs), and their consumption has recently increased. Some manufacturers use a praseodymium (Pr)–Nd alloy called didymium (Di) for the magnets instead of Nd metal. Because their relatively low Curie temperature is a drawback for Nd–Fe–B magnets, dysprosium (Dy) is added to the grain boundaries of the Nd–Fe–B magnets to maintain the superior coercive force even at elevated operation temperatures above 473 K for high-performance motors used in EVs and HEVs.

Recently, the global concerns for RE magnets are the resource and environmental problems. In 2011, China had 50% of the proven RE reserves and produced over 97% of the global RE supply,[1] which induced a sharp increase in the price of REs and supply problems for the magnets in 2010–2012. In addition, severe environmental pollution has been caused by mining, e.g., a large amount of radioactive wastes and water pollution have been produced because of insufficient antipollution measures. Under these circumstances, the recycling and waste management of Nd–Fe–B magnet scraps are urgent tasks. The conventional wet processes of RE recycling for Nd–Fe–B magnet scraps have several disadvantages such as multistep and complicated processes, high environmental loads, and large energy consumption. As new recycling methods,

pyrometallurgical processes have been investigated: chemical vapour transport,[2] selective reduction,[3] molten salt electrolysis,[4] ionic liquid electrolysis,[5] and extraction to molten metal,[6] salt,[7] and slag.[8] Among these processes, a simple and environmentally friendly process is desired for recycling Pr, Nd, and Dy from the used magnets that will be discarded from EVs and HEVs in the near future.

We have proposed a new separation and recovery process for RE elements from magnet scraps using molten salt electrochemistry utilizing an alloy diaphragm.[9–15] In the proposed process, two molten salt electrolytes are separated by an RE–iron group (IG) alloy diaphragm. Scraps of RE magnets are used as an anode to dissolve RE elements into the molten salt in the anode chamber, and then, Pr, Nd, and Dy are separated using the differences in both the formation potentials and formation rates of the RE–IG alloys. The RE metals are separately recovered via electrodeposition onto the cathode in the cathode chamber. We have already reported the electrochemical behavior of RE elements (RE = Pr, Nd, and Dy) and the formation of RE–Ni alloys in molten LiF–CaF_2–REF_3 salts at 1123 K[10–12,15] and molten NaCl–KCl–$RECl_3$ salts at 973 K.[13–15] Concerning the LiF–CaF_2 eutectic melt, Nourry *et al.* also reported the formations of Nd–Ni alloys.[16,17] For the application of the process, investigations not only of the behaviors of each element but also of the separation between Pr, Nd, and Dy are essential. Konishi *et al.* have already reported selective formation of RE–Ni alloys using the same technique in a molten LiCl–KCl melt at 723 K and achieved a high separation mass ratio of Dy/Nd = 72 in the alloy samples.[18–20]

In the present study, to verify the separation of RE elements, the formation of RE–Ni alloys (RE = Pr, Nd, and Dy) was further investigated in molten NaCl–KCl–$RECl_3$ salts at 973 K. Because the NaCl–KCl melts have higher operation temperatures compared

with LiCl–KCl melts (723 K), faster separation was expected. First, the alloy formation rates were compared between Pr, Nd, and Dy. Second, the optimum electrolysis potential was investigated for selective alloy formation. Finally, the reaction mechanism was discussed by comparison with the previously reported separation behavior in LiCl–KCl molten salt.

2. Experimental

The details of the experimental setup and procedure have already been reported elsewhere.[13] Two hundred grams of the mixture of NaCl and KCl with a consolute composition (NaCl:KCl = 50.6:49.4 mol%, m.p. = 930 K[21]) were loaded into a glassy carbon crucible. The experiments were performed under a dried and deoxygenated Ar atmosphere in a glove box at 973 K. Powdery $RECl_3$ was added directly into the melts as a RE ion source, and a Ni plate (5 mm × 8 mm × 0.2 mm) was used as the working electrode. A glassy carbon rod was used as the counter electrode. A Ag wire (1-mm diameter) immersed in molten NaCl–KCl containing 1.0 mol% AgCl set in a mullite tube (o.d. 6 mm × i.d. 4 mm × length 500 mm, 56% Al_2O_3–40% SiO_2; HB grade, Nikkato Corp.), which exhibits Na^+ ion conduction owing to the impurity of Na_2O, was used for the Ag^+/Ag reference electrode.[13] The potential of the reference electrode was occasionally calibrated with reference to the potential of a Na^+/Na dynamic reference electrode, which was prepared by the electrodeposition of Na metal on a Mo wire.[13] All the potentials in this study are given with reference to this Na^+/Na electrode potential. The prepared RE–Ni alloy samples were analyzed by scanning electron microscopy

(SEM) using secondary electrons, energy-dispersive X-ray spectroscopy (EDX), and inductively coupled plasma-atomic emission spectroscopy (ICP-AES, Thermo Scientific、iCAP 6200 Duo). The alloy samples prepared by electrolysis of Ni plates were usually covered with solidified salts. Before analysis by SEM/EDX, the samples were treated as follows.[13] They were first immersed in ethylene glycol (Wako Pure Chemical Co. Ltd., 99.5%) to remove chloride salts at room temperature for more than 1 day. After washing with acetone, the samples were embedded in acrylic resin (VariDur®, Buehler) and polished with emery paper (#240, 400, 600, 1000, and 2000).

3. Results and Discussion

3.1 Formation potentials of RE–Ni alloys

Table 1 compares the formation reactions and corresponding potentials for RE–Ni alloys and RE metals in molten NaCl–KCl–$RECl_3$ (0.50 mol%) at 973 K (RE = Pr, Nd, and Dy) that have already been reported.[13–15] The separation of Pr and Nd using potential control is suggested to be difficult because of the very similar formation potentials. However, the separation of Pr and Nd is not necessary because the Pr–Nd alloy called Di can be directly recycled into magnets without separation. However, the separation of Dy from Pr and Nd is highly expected at 0.39 V–0.48 V (vs. Na^+/Na). In this potential range, the $RENi_2$ phase forms for the Dy–Ni system, and the $RENi_3$ or RE_2Ni_7 phases form for both the Pr–Ni and Nd–Ni systems. Because the formation rates of RE-deficient RE–Ni phases such as $RENi_3$, RE_2Ni_7, and $RENi_5$ are very slow and that of RE-abundant phase

of $RENi_2$ is fast in molten LiCl–KCl at 723 K,[22–24] the selective fast formation of $DyNi_2$ at these potentials is also expected in a NaCl–KCl melt.

*** Table 1 ***

3.2 Formation rates of RE–Ni alloys

The formation rates of RE–Ni alloys were compared among the samples prepared by potentiostatic electrolysis of Ni plate electrodes at 0.42 V in molten NaCl–KCl at 973 K containing either 0.50 mol% $PrCl_3$, 0.50 mol% $NdCl_3$, or 0.50 mol% $DyCl_3$. As indicated in the previous section, the formations of $PrNi_3$, $NdNi_3$, and $DyNi_2$ are expected at this potential. The thickness of the alloy layer was measured from cross-sectional SEM images, as shown in Fig. 1 ((a) Pr–Ni, (b) Nd–Ni, and (c) Dy–Ni). The thickness of the Pr–Ni alloy layer is 2 μm, and its composition analyzed by EDX is Pr:Ni = 16.1:83.9 at%. The lower Pr concentration compared with the theoretical value of $PrNi_3$ is caused by the inclusion of the Ni substrate in the EDX analysis area (2–3 μm in diameter). The thickness and composition are 4 μm and Nd:Ni = 18.1:81.9 at% for the Nd–Ni alloy, and 50 μm and Dy:Ni = 34.1:65.9 at% for the Dy–Ni alloy, respectively. The formation rate of $DyNi_2$ is one order of magnitude faster than those of the Pr–Ni and Nd–Ni alloys, which suggests the possibility of efficient separation of Dy from Pr and Nd in the proposed electrochemical process.

*** Fig. 1 ***

3.3 Selective formation rates of RE–Ni alloys

Based on the above results, selective formation of RE–Ni alloys (RE = Pr, Nd, and Dy) was examined in molten NaCl–KCl at 973 K containing (1) both 0.50 mol% $NdCl_3$ and 0.50 mol% $DyCl_3$, and (2) 0.50 mol% $PrCl_3$, 0.50 mol% $NdCl_3$, and 0.50 mol% $DyCl_3$. According to Table 1 and Fig. 1, the formation of RE–Ni alloys is expected to preferentially occur for Dy–Ni alloys at 0.39–0.48 V. Thus, electrolysis potentials of 0.35, 0.42, 0.45, and 0.50 V were selected. After the electrolysis for 60 min, the thickness and composition of the alloy layers were analyzed using SEM/EDX.

Figures 2 and 3 present cross-sectional SEM images of the obtained alloys in the molten NaCl–KCl–$NdCl_3$–$DyCl_3$ and NaCl–KCl–$PrCl_3$–$NdCl_3$–$DyCl_3$ systems, respectively. In both molten salts, the current transient and thickness of alloy layer were almost the same at the same potential. The thickness increases as the potential becomes negative: 80–100 μm (0.35 V), 60 μm (0.42 V), 10–30 μm (0.45 V), and 3 μm (0.50 V). Even in the range of 0.39–0.48 V, the growth rate of alloy is faster at more negative potentials as observed in Fig. 4.

*** Fig. 2 ***

*** Fig. 3 ***

*** Fig. 4 ***

Table 2 summarizes the compositions of the formed alloy layers determined by EDX. Elements except for REs and Ni, such as O and Cl, were not detected. For all the samples, the compositions are almost the same at any positions of the formed RE–Ni alloy layers. Importantly, the concentration of Dy is always highest among all the RE elements. Except for the samples at 0.50 V, the composition of all the samples corresponds to the $RENi_2$ phase, which agrees with our expectation. At the most negative potential of 0.35 V,

the concentrations of Pr and Nd become high, whereas that of Dy decreases, which also agrees with our expectation. As planned, low concentrations of Pr and Nd and high concentrations of Dy were achieved at 0.42 and 0.45 V. This result is explained by the selective formation of the $DyNi_2$ phase at these potentials. At 0.50 V, the samples have compositions suggesting the formation of a mixture of RE_2Ni_7 and $RENi_5$ phases, which is different from the expected phase of $RENi_3$.

In this study, the separation factor is defined as $\{x_{Dy}/(x_{Pr} + x_{Nd})\}_{alloy}$, where x_{Dy}, x_{Pr}, and x_{Dy} are the atomic compositions of Dy, Pr, and Nd for the RE–Ni alloy, respectively. Here, the value of x_{Pr} in the system containing no $PrCl_3$ is considered to be zero. The calculated separation factors from the EDX analysis are also listed in Table 2 and plotted against the potential in Fig. 5. As expected, a high separation factor is obtained between 0.39 and 0.48 V. In the molten NaCl–KCl–$NdCl_3$–$DyCl_3$, the factors are 11.6–26.0 (avg. 18.8) at 0.42 V and 23.7 at 0.45 V. In the molten NaCl–KCl–$PrCl_3$–$NdCl_3$–$DyCl_3$, the values are 5.5–14.9 (avg. 9.9) at 0.42 V and 22.9 at 0.45 V. The factor was also determined to be 15.1 using ICP-AES for the sample at 0.42 V, which agrees with the result determined by EDX. The scattering of the data is likely due to the different sequence of $RECl_3$ addition to the melt in the different experiments. The actual concentration of the $RECl_3$, which was added first, appears to be slightly less than 0.50 mol% from the reaction with the residual moisture in the molten salt to form REOCl. Thus, the concentration of that RE element tends to be low in the alloy samples. Even with the scattering of the data, these results experimentally confirm the feasibility of separation of Dy from Pr and Nd by electrochemical alloy formation.

*** Table 2 ***

*** Fig. 5 ***

3.4 Mechanism for formation of RE–Ni alloys

The formation rate of the $RENi_2$ alloy layer in the NaCl–KCl–$RECl_3$ melt at 973 K is plotted in Fig. 6 against the overvoltage from the $DyNi_2$/$DyNi_3$ equilibrium potential (0.48 V vs. Na^+/Na). The rate proportionally increases with the overvoltage with a slope of 0.9 μm h^{-1} mV^{-1}. The formation rate of $DyNi_2$ in molten LiCl–KCl–0.50 mol%$DyCl_3$ at 700 K reported in Ref. 25 is also plotted in the same manner. The formation rate also proportionally increases with the overvoltage with a slope of 0.1 μm h^{-1} mV^{-1}. Concerning the formation kinetics of the $RENi_2$ alloy layer, it was reported from the current transients and cross-sectional SEM images that its growth changes from following a parabolic rate law during the initial period to following a linear rate law afterwards, which is explained by the existence of the outer and inner $DyNi_2$ layers.[25] A linear growth rate was also reported for $NdNi_2$ in molten LiCl–KCl–0.50 mol%$NdCl_3$.[18] The reaction kinetics was one order of magnitude faster in molten NaCl–KCl at higher temperature.

The difference of the separation factors between NaCl–KCl–$NdCl_3$–$DyCl_3$ and NaCl–KCl–$PrCl_3$–$NdCl_3$–$DyCl_3$ in Fig. 5 is explained by the composition of the molten salt as follows. Figure 7 plots the separation factor, $\{x_{Dy}/(x_{Pr} + x_{Nd})\}_{alloy}$, against the molar ratio of Dy to (Pr + Nd) in the molten salt, $\{x_{Dy}/(x_{Pr} + x_{Nd})\}_{molten\ salt}$, at the potential of selective $DyNi_2$ formation. Here, the reported separation factor in the LiCl–KCl melt is also plotted after the recalculation from weight to atomic ratio.[18–20] As observed in the plots, there is a proportional relationship,

$$\left\{\frac{x_{\mathrm{Dy}}}{x_{\mathrm{Nd}}+x_{\mathrm{Pr}}}\right\}_{\mathrm{alloy}} = p_{a/m} \cdot \left\{\frac{x_{\mathrm{Dy}}}{x_{\mathrm{Nd}}+x_{\mathrm{Pr}}}\right\}_{\mathrm{molten\ salt}}, \quad (1)$$

where $p_{\mathrm{a/m}}$ is an electrochemical partition coefficient, which indicates the enrichment factor of Dy from the molten salts to RE–Ni alloy. That is, the separation factor is directly related to the molar ratio of Dy to other RE elements in molten salts. The values of $p_{\mathrm{a/m}}$ are 19.1 at 0.42 V (vs. Na^+/Na) in molten NaCl–KCl at 973 K and 85.9 at 0.65 V (vs. Li^+/Li) in molten LiCl–KCl at 723 K. The existence of Li^+ cations[24] and/or the wide potential range for selective formation would result in the larger $p_{\mathrm{a/m}}$ of high separation ability in LiCl–KCl.

Considering the actual operation of selective Dy recovery by the proposed alloy diaphragm method, although the enrichment of Dy proceeds with a high separation factor in the initial stage, the separation factor decreases in the long-term operation because of the lowered Dy concentration in the anode chamber. Thus, for continuous recovery of Dy with a high separation factor, the molar ratio of $\{x_{\mathrm{Dy}}/(x_{\mathrm{Pr}} + x_{\mathrm{Nd}})\}_{\mathrm{molten\ salt}}$ in the anode chamber should not become too low. As illustrated in Fig. 8, simultaneous or intermittent electrolytic removal of Pr and Nd from the anode chamber is a possible solution. Here, didymium (Pr–Nd alloy) and Dy metal are separately recovered at the cathode in the anode chamber and the cathode in the cathode chamber, respectively. The produced didymium can be directly recycled into magnets without their separation.

*** Fig. 6 ***

*** Fig. 7 ***

*** Fig. 8 ***

Conclusions

With the aim of establishing a recycling process for used Nd magnets containing Pr and Dy, electrochemical separation of Pr, Nd, and Dy utilizing RE–Ni alloy formation was investigated in a molten NaCl–KCl–$RECl_3$ system at 973 K. Alloy samples prepared by potentiostatic electrolysis were analyzed using SEM/EDX. The electrolysis potential range for effective separation of Dy from Pr and Nd was suggested to be 0.39–0.48 V (vs. Na^+/Na). In this potential range, the formation of the Dy–Ni alloy layer proceeded 10 times faster than those of Pr–Ni and Nd–Ni. Moreover, the formation rate increased when the potential became more negative. The separation factor defined as $\{x_{Dy}/(x_{Pr} + x_{Nd})\}_{alloy}$ had high values of 9.9 and 22.9 at 0.42 and 0.45 V, respectively. Considering the actual operation of the proposed alloy diaphragm method, periodic removal of Pr and Nd from the anode chamber was suggested to be necessary to maintain the high separation factor of Dy.

Acknowledgments

The authors acknowledge Dr. Hirokazu Konishi at Osaka University for valuable discussions. ICP analysis was performed with the assistance of Sumitomo Electric Industries, Ltd.

References

1. U.S. Geological Survey, Mineral Commodity Summaries 2012.
2. K. Murase, K. Machida, and G. Adachi, *J. Alloy. Compd*., **217**, 218 (1995).
3. T. Uda, K. T. Jacob, and M. Hirasawa, *Science*, **289**, 2326 (2000).
4. T. Oishi, H. Konishi, and T. Nohira, *Japanese Patent Applications*, JPA 2009-287119 (2009).
5. M. Matsumiya, H. Kondo, A. Kurachi, K. Tsunashima, and S. Kodama, *J. Japan Inst. Metals*, **75**, 607 (2011).
6. O. Takeda, T. H. Okabe, and Y. Umetsu, *J. Alloy. Compd.*, **379**, 305 (2004).
7. S. Shirayama and T. H. Okabe, Proc. on PMP III, 469 (TMS, Warrendale, 2009).
8. H. Sekimoto, T. Kubo, and K. Yamaguchi, *J. MMIJ*, **130**, 494 (2014) (in Japanese).
9. T. Oishi, H. Konishi, T. Nohira, M. Tanaka, and T. Usui, *Kagaku Kogaku Ronbunshu*, **36**, 299 (2010) (in Japanese).
10. T. Nohira, S. Kobayashi, K. Kobayashi, R. Hagiwara, T. Oishi, and H. Konishi, *ECS Trans.*, **33**, 205 (2010).
11. S. Kobayashi, K. Kobayashi, T. Nohira, R. Hagiwara, T. Oishi, and H. Konishi, *J. Electrochem. Soc.*, **158**, E142 (2011).
12. T. Nohira, S. Kobayashi, K. Kobayashi, K. Yasuda, R. Hagiwara, T. Oishi, and H. Konishi, *J. Electrochem. Soc*., **159**, E193 (2012).
13. K. Yasuda, S. Kobayashi, T. Nohira, and R. Hagiwara, *Electrochim. Acta*, **92**, 349 (2013).

14. K. Yasuda, S. Kobayashi, T. Nohira, and R. Hagiwara, *Electrochim. Acta*, **106**, 293 (2013).
15. K. Yasuda, K. Kondo, T. Nohira, and R. Hagiwara, *J. Electrochem. Soc.*, **161**, D3097 (2014).
16. C. Nourry, L. Massot, P. Chamelot, and P. Taxil, *J. New Mater. Electrochem. Syst*., **10**, 117 (2007).
17. C. Nourry, L. Massot, P. Chamelot, and P. Taxil, *J. Appl. Electrochem*., **39**, 927 (2009).
18. H. Konishi, H. Ono, T. Nohira, and T. Oishi, *ECS Trans.*, **50**, 463 (2012).
19. T. Nohira, S. Kobayashi, K. Kondo, K. Yasuda, R. Hagiwara, T. Oishi, and H. Konishi, *ECS Trans.*, **50**, 473 (2012).
20. H. Konishi, H. Ono, E. Takeuchi, T. Nohira, and T. Oishi, *ECS Trans.*, **64**, 593 (2014).
21. J. M. Sangster and A. D. Pelton, *J. Phys. Chem. Ref. Data*, **16**, 509 (1987).
22. H. Konishi, T. Nohira, and Y. Ito, *J. Electrochem. Soc*., **148**, C506 (2001).
23. T. Iida, T. Nohira, and Y. Ito, *Electrochim. Acta*, **46**, 2537 (2001).
24. T. Nohira, H. Kambara, K. Amezawa, and Y. Ito, *J. Electrochem. Soc*., **152**, C183 (2005).
25. H. Konishi, T. Nohira, and Y. Ito, *Electrochim. Acta*, **48**, 563 (2003).

List of Table and Figure Captions

Table 1 Formation reactions and corresponding potentials for RE–Ni alloys and RE metals in molten NaCl–KCl–0.50 mol%$RECl_3$ at 973 K (RE = Pr, Nd, and Dy).[13–15]

Table 2 Alloy composition and separation factors of the samples obtained by the potentiostatic electrolysis of Ni plate electrodes at each potential for 60 min in molten NaCl–KCl–0.50 mol% $NdCl_3$–0.50 mol% $DyCl_3$(–0.50 mol% $PrCl_3$) systems at 973 K.

Figure 1 Cross-sectional SEM images of the samples obtained by the potentiostatic electrolysis of Ni plate electrodes at 0.42 V for 60 min in molten (a) NaCl–KCl–0.50 mol%$PrCl_3$, (b) NaCl–KCl–0.50 mol%$NdCl_3$, and (c) NaCl–KCl–0.50 mol%$DyCl_3$ and at 973 K.

Figure 2 Cross-sectional SEM images of the samples obtained by the potentiostatic electrolysis of Ni plate electrodes at (a) 0.35, (b) 0.42, (c) 0.45, and (d) 0.50 V for 60 min in molten NaCl–KCl–0.50 mol%$NdCl_3$–0.50 mol%$DyCl_3$ system at 973 K.

Figure 3 Cross-sectional SEM images of the samples obtained by the potentiostatic electrolysis of Ni plate electrodes at (a) 0.35, (b) 0.42, (c) 0.45, and (d) 0.50 V for 60 min in molten NaCl–KCl–0.50 mol%$PrCl_3$–0.50 mol%$NdCl_3$–0.50 mol%$DyCl_3$ system at 973 K.

Figure 4 Formation rate of alloy layers of the samples obtained by the potentiostatic electrolysis of Ni plate electrodes at each potential for 60 min in molten NaCl–KCl–0.50 mol%$NdCl_3$–0.50 mol%$DyCl_3$(–0.50 mol%$PrCl_3$) system at 973 K.

Figure 5 Separation factor of the samples obtained by the potentiostatic electrolysis of Ni plate electrodes at each potential for 60 min in molten NaCl–KCl–0.50 mol%$NdCl_3$–0.50 mol%$DyCl_3$(–0.50 mol%$PrCl_3$) system at 973 K.

Figure 6 Formation rate of $RENi_2$ alloy layer at various overvoltages from $DyNi_2$/$DyNi_3$ equilibrium potential in NaCl–KCl–0.50 mol%$NdCl_3$–0.50 mol%$DyCl_3$(–0.50 mol%$PrCl_3$) melt at 973 K and LiCl–KCl–0.50 mol%$DyCl_3$ melt at 700 K.[25]

Figure 7 Composition ratio, $x_{Dy}/(x_{Nd} + x_{Pr})$, in molten salt and alloy layer. The alloy samples were prepared at 0.42 V vs. Na^+/Na in molten NaCl–KCl–0.50 mol%$NdCl_3$–0.50 mol%$DyCl_3$(–0.50 mol%$PrCl_3$) system at 973 K and at 0.65 V vs. Li^+/Li in molten LiCl–KCl–0.50 mol%$NdCl_3$–0.50 mol%$DyCl_3$(–0.50 mol%$PrCl_3$) system at 723 K.[18–20]

Figure 8 Separation and recovery process of RE metals from scraps using molten salt and alloy diaphragm, which maintains a high separation ability of Dy in a continuous operation.

Table 1 Formation reactions and corresponding potentials for RE–Ni alloys and RE metals in molten NaCl–KCl–0.50 mol%$RECl_3$ at 973 K (RE = Pr, Nd, and Dy).[13–15]

Formation reaction	Potential vs. Na^+/Na / V		
	RE = Pr	RE = Nd	RE = Dy
$5\ Ni + RE(III) + 3\ e^- \rightleftharpoons RENi_5$	0.78	0.79	0.87
$7/3\ RENi_5 + RE(III) + 3\ e^- \rightleftharpoons 5/3\ RE_2Ni_7$	0.52	0.55	0.72
$3\ RE_2Ni_7 + RE(III) + 3\ e^- \rightleftharpoons 7\ RENi_3$	0.45	0.48	0.64
$2\ RENi_3 + RE(III) + 3\ e^- \rightleftharpoons 3\ RENi_2$	0.38	0.39	0.48
$RE(III) + 3\ e^- \rightleftharpoons RE$	0.23	0.22	0.24

Table 2 Alloy composition and separation factors of the samples obtained by the potentiostatic electrolysis of Ni plate electrodes at each potential for 60 min in molten NaCl–KCl–0.50 mol% $NdCl_3$–0.50 mol% $DyCl_3$(–0.50 mol% $PrCl_3$) systems at 973 K.

Additive	Potential vs. Na^+/Na / V	Alloy composition [a] / at%				Separation factor
		Pr	Nd	Dy	Ni	
$NdCl_3$ and $DyCl_3$	0.35	–	7.8	25.1	67.1	3.2 [b]
	0.42	–	1.2	31.2	67.6	26.0 [b]
		–	2.7	31.4	65.9	11.6 [b]
	0.45	–	1.4	33.3	65.3	23.7 [b]
	0.50	–	1.8	17.9	80.3	9.9 [b]
$PrCl_3$, $NdCl_3$ and $DyCl_3$	0.35	6.5	8.6	15.5	69.4	1.0 [c]
	0.42	0.7	1.3	29.8	68.2	14.9 [c]
		1.2	2.0	29.9	66.9	9.3 [c]
		1.9	3.2	27.9	67.0	5.5 [c]
		–	–	–	–	(15.1 [d])
	0.45	0.6	0.8	32.1	66.5	22.9 [c]
	0.50	0.7	1.1	15.9	82.3	8.8 [c]

a: Detemined by EDX
b: x_{Dy} / x_{Nd}
c: $x_{Dy} / (x_{Pr} + x_{Nd})$
d: Detemined by ICP-AES

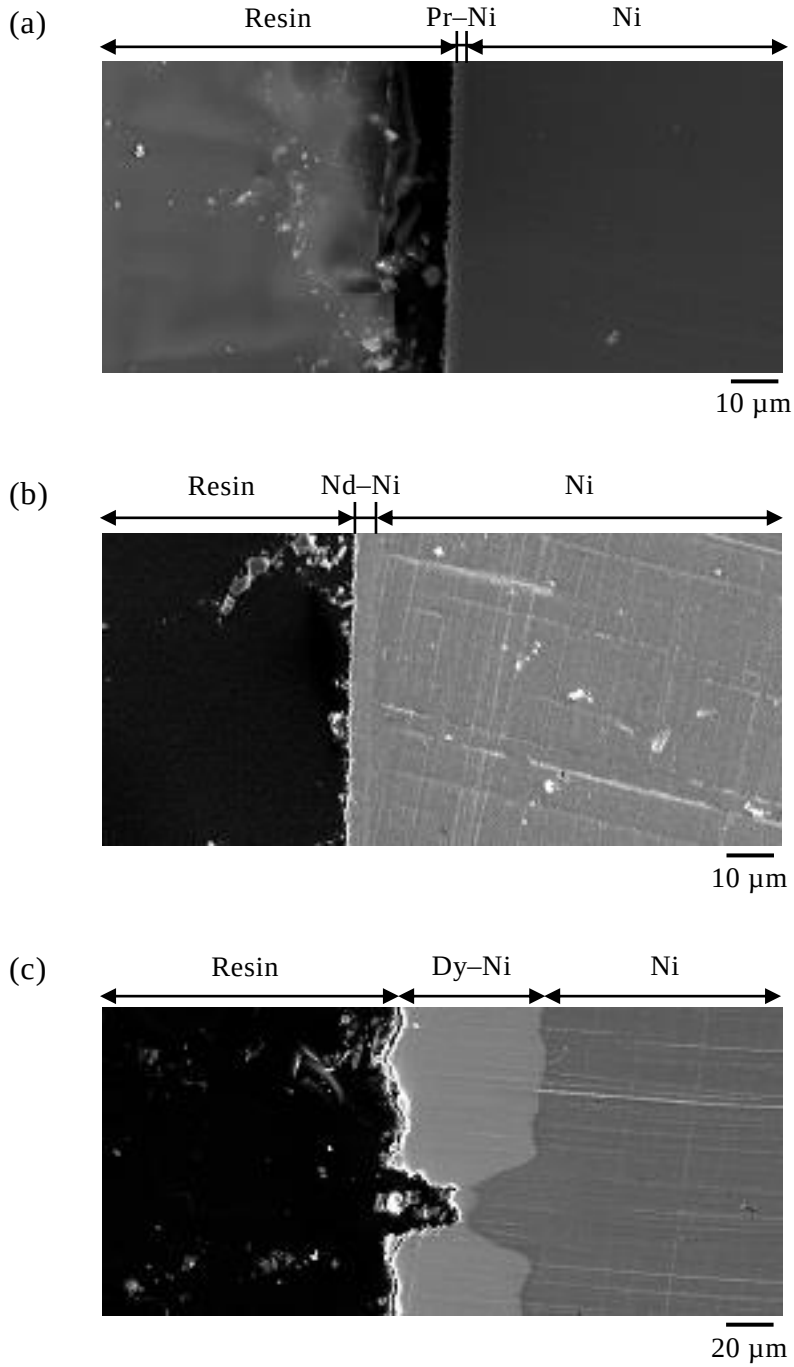

Figure 1 Cross-sectional SEM images of the samples obtained by the potentiostatic electrolysis of Ni plate electrodes at 0.42 V for 60 min in molten (a) NaCl–KCl–0.50 mol%$PrCl_3$, (b) NaCl–KCl–0.50 mol%$NdCl_3$, and (c) NaCl–KCl–0.50 mol%$DyCl_3$ at 973 K.

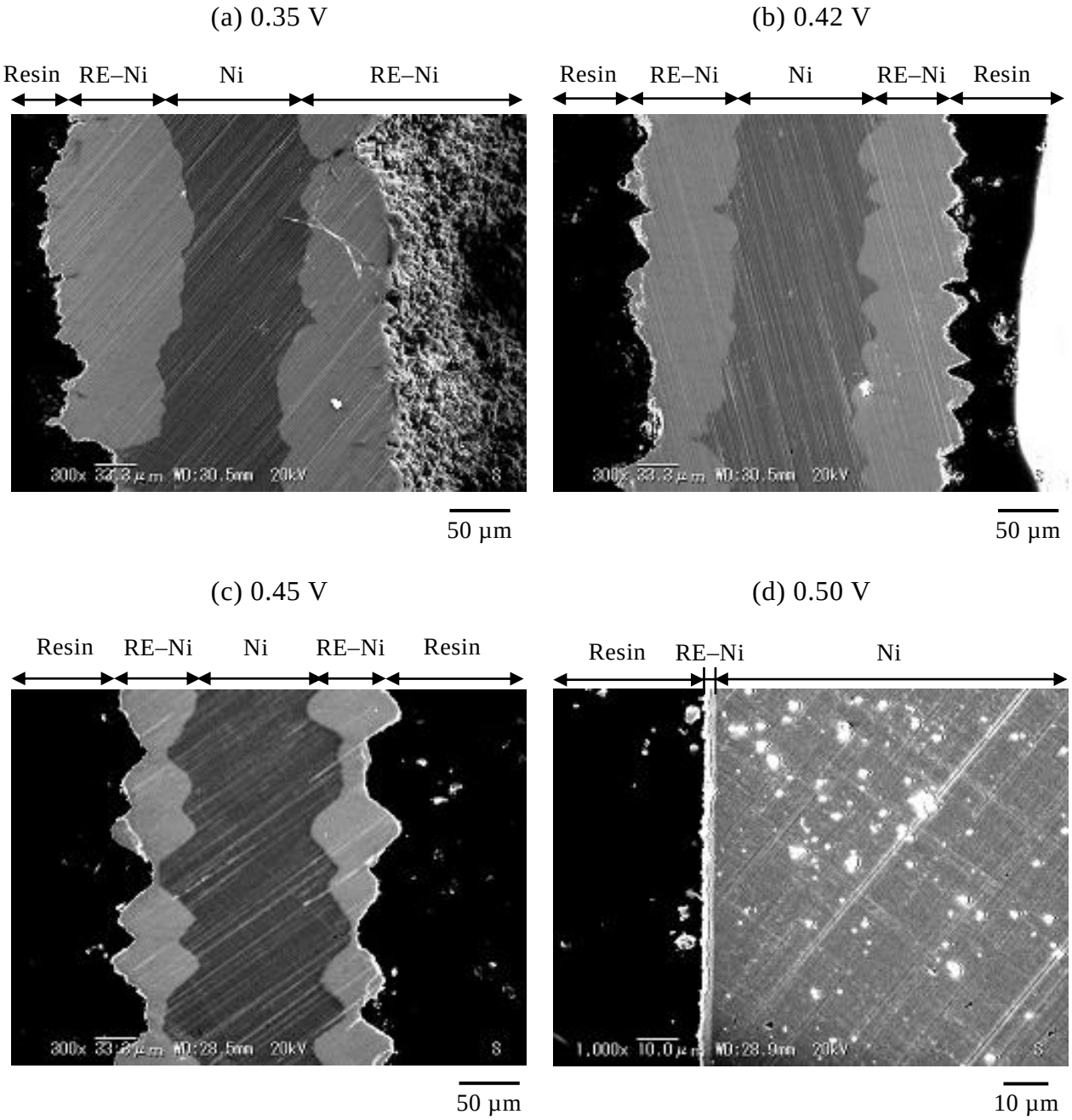

Figure 2 Cross-sectional SEM images of the samples obtained by the potentiostatic electrolysis of Ni plate electrodes at (a) 0.35, (b) 0.42, (c) 0.45, and (d) 0.50 V for 60 min in molten NaCl–KCl–0.50 mol%$NdCl_3$–0.50 mol%$DyCl_3$ system at 973 K.

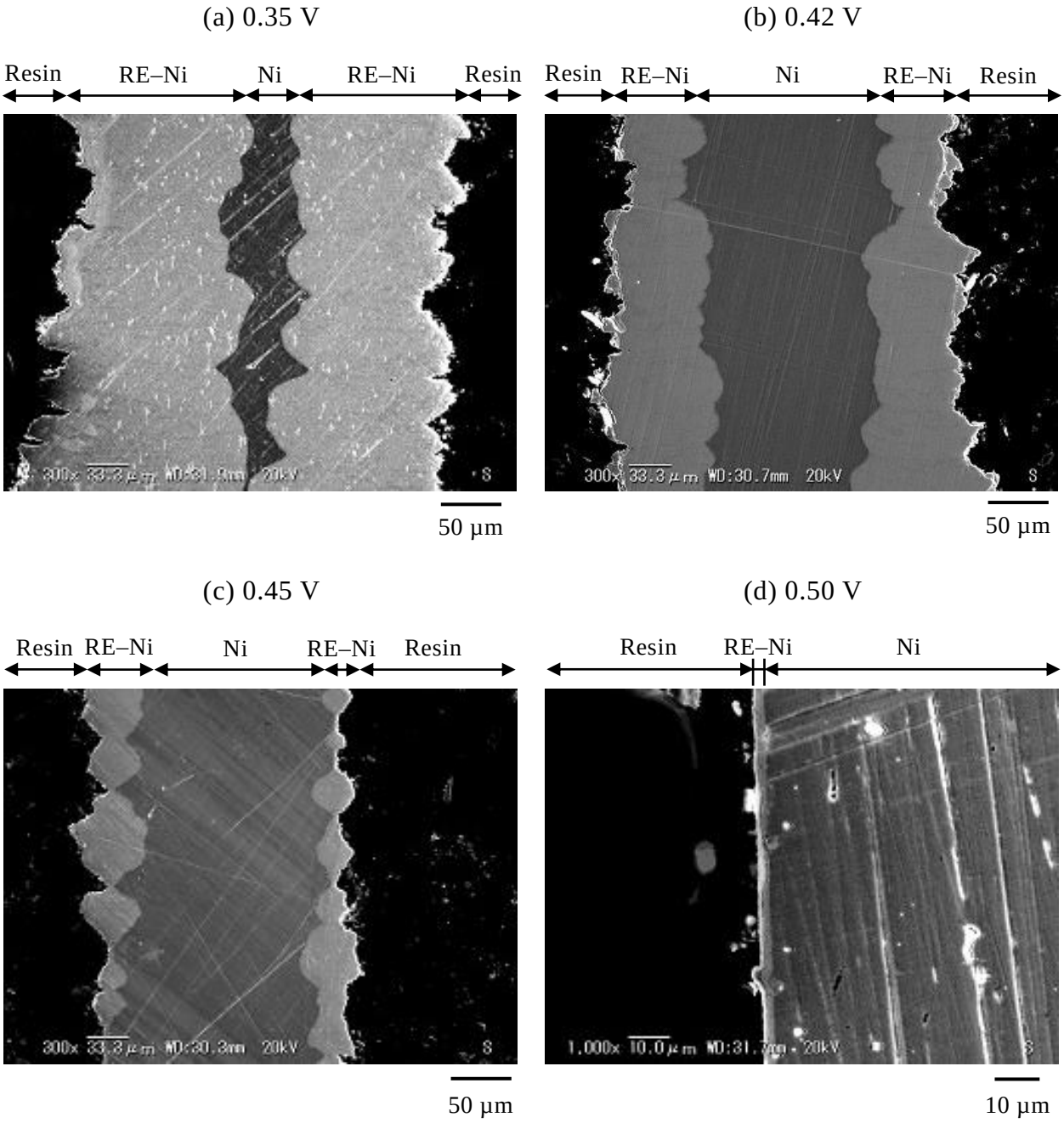

Figure 3 Cross-sectional SEM images of the samples obtained by the potentiostatic electrolysis of Ni plate electrodes at (a) 0.35, (b) 0.42, (c) 0.45, and (d) 0.50 V for 60 min in molten NaCl–KCl–0.50 mol%$PrCl_3$–0.50 mol%$NdCl_3$–0.50 mol%$DyCl_3$ system at 973 K.

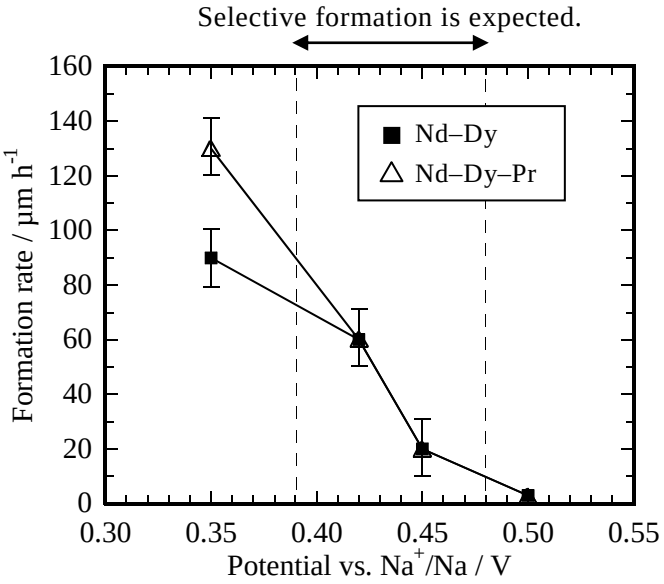

Figure 4 Formation rate of alloy layers of the samples obtained by the potentiostatic electrolysis of Ni plate electrodes at each potential for 60 min in molten NaCl–KCl–0.50 mol%$NdCl_3$–0.50 mol%$DyCl_3$(–0.50 mol%$PrCl_3$) system at 973 K.

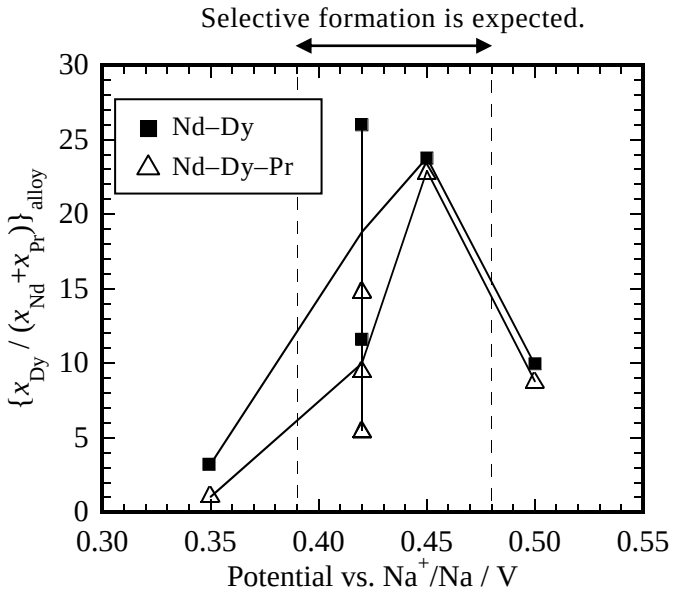

Figure 5 Separation factor of the samples obtained by the potentiostatic electrolysis of Ni plate electrodes at each potential for 60 min in molten NaCl–KCl–0.50 mol%$NdCl_3$–0.50 mol%$DyCl_3$(–0.50 mol%$PrCl_3$) system at 973 K.

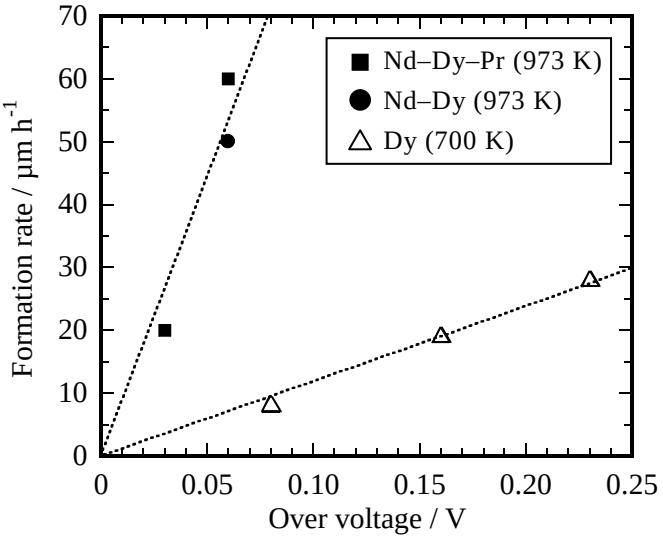

Figure 6 Formation rate of $RENi_2$ alloy layer at various overvoltages from $DyNi_2/DyNi_3$ equilibrium potential in NaCl–KCl–0.50 mol%$NdCl_3$–0.50 mol%$DyCl_3$(–0.50 mol%$PrCl_3$) melt at 973 K and LiCl–KCl–0.50 mol%$DyCl_3$ melt at 700 K.[25]

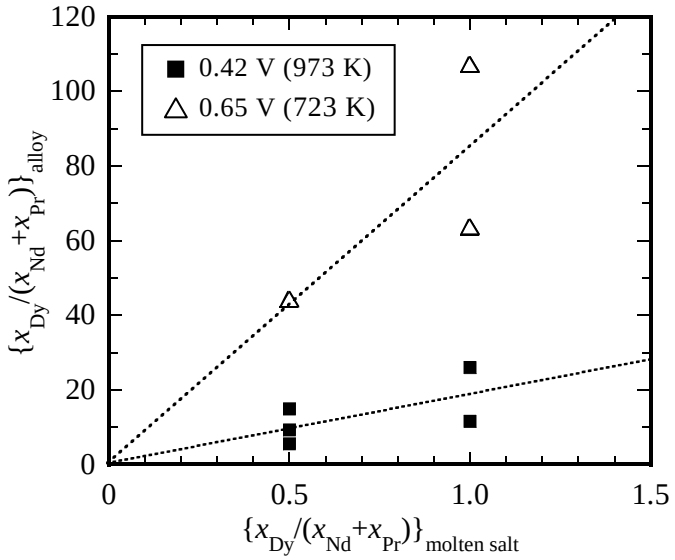

Figure 7 Composition ratio, $x_{Dy}/(x_{Nd} + x_{Pr})$, in molten salt and alloy layer. The alloy samples were prepared at 0.42 V vs. Na^+/Na in molten NaCl–KCl–0.50 mol%$NdCl_3$–0.50 mol%$DyCl_3$(–0.50 mol%$PrCl_3$) system at 973 K and at 0.65 V vs. Li^+/Li in molten LiCl–KCl–0.50 mol%$NdCl_3$–0.50 mol%$DyCl_3$(–0.50 mol%$PrCl_3$) system at 723 K.[18–20]

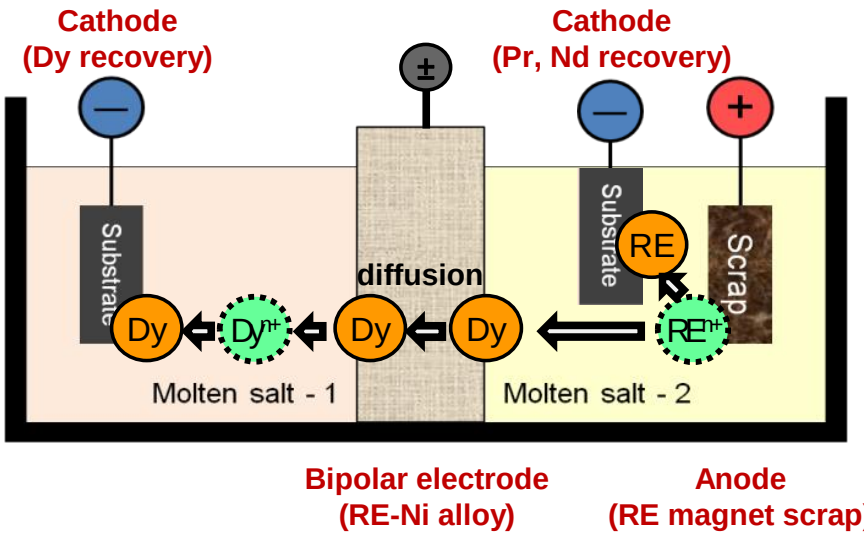

Figure 8 Separation and recovery process of RE metals from scraps using molten salt and alloy diaphragm which maintains a high separation ability of Dy in a continuous operation.